arXiv:hep-ph/0010018v1 3 Oct 2000

Production of Charginos, Neutralinos, and Third Generation Sfermions at an e^+e^- Linear Collider

A. Bartl,[1] H. Eberl,[2] H. Fraas,[3] S. Kraml,[2] W. Majerotto,[2] G. Moortgat–Pick,[4] W. Porod [5]

[1] *Institut für Theoretische Physik, Universität Wien, A–1090 Vienna, Austria*

[2] *Inst. f. Hochenergiephysik, Österr. Akademie d. Wissenschaften, A–1050 Vienna, Austria*

[3] *Institut für Theoretische Physik, Universität Würzburg, D–97074 Würzburg, Germany*

[4] *DESY, Deutsches Elektronen–Synchrotron, D–22603 Hamburg, Germany*

[5] *Inst. de Física Corpuscular (IFIC), CSIC, E–46071 València, Spain*

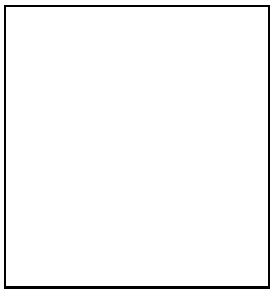

We discuss the production of neutralinos, charginos, and third generation sfermions in e^+e^- annihilation in the energy range $\sqrt{s} = 0.2 - 1$ TeV. We present numerical predictions within the Minimal Supersymmetric Standard Model for the cross sections and study the importance of beam polarization for the determination of the underlying SUSY parameters.

1 Introduction

The search for supersymmetric (SUSY) particles will be one of the main goals of a future e^+e^- linear collider with an energy range $\sqrt{s} = 0.5 - 1$ TeV. Such an e^+e^- linear collider will also be very well suited for the precision determination of the parameters of the underlying SUSY model. This will be necessary to find out the mechanisms of SUSY breaking and electroweak symmetry breaking.

In this contribution we summarize the results of our recent phenomenological studies on the production of charginos, neutralinos and third generation sfermions in e^+e^- annihilation at energies between $\sqrt{s} = 200$ GeV and 1 TeV [1,2]. We consider the effects of both e^- and e^+ beam polarizations. Polarizing both beams can be advantageous for three reasons: (i) One can obtain higher cross sections. (ii) By measuring appropriate observables one can get additional information on the SUSY parameters. (iii) One can reduce the background. We perform our calculations in the Minimal Supersymmetric Standard Model (MSSM) [3] and study the SUSY parameter dependence of cross sections and decay rates.

2 Production of Charginos and Neutralinos

The masses and couplings of neutralinos and charginos are determined by their mixing matrices. The explicit forms of the mixing matrices and their dependences on the SUSY parameters are given, e. g., in [4]. Chargino pair production proceeds via γ and Z exchange in the s–channel and $\tilde{\nu}_e$ exchange in the t–channel. The amplitude for $e^+e^- \to \tilde{\chi}_i^0\tilde{\chi}_j^0$ has contributions from Z exchange in the s–channel and $\tilde{e}_L$ and $\tilde{e}_R$ exchanges in the t– and u–channel. As an example we show in Fig. 1 contour plots of the cross section of $e^+e^- \to \tilde{\chi}_1^0\tilde{\chi}_2^0$ as a function of the longitudinal electron and positron beam polarizations $\mathcal{P}_-$ and $\mathcal{P}_+$, at $\sqrt{s} = 230$ GeV. The SUSY parameters we have chosen as $M_2 = 152$ GeV, $\mu = 316$ GeV, $\tan\beta = 3$. The corresponding neutralino masses are $m_{\tilde{\chi}_1^0} = 71$ GeV and $m_{\tilde{\chi}_2^0} = 130$ GeV. The masses of the exchanged selectrons we have taken as $m_{\tilde{e}_R} = 132$ GeV and $m_{\tilde{e}_L} = 176$ GeV in Fig. 1 a, whereas in Fig. 1 b we have changed the value of $m_{\tilde{e}_L}$ into $m_{\tilde{e}_L} = 500$ GeV. As can be seen, the cross section depends sensitively on the e^- and e^+ beam polarizations. In Fig. 1b the cross section for left–polarized e^- beams is much smaller than in Fig. 1a, because the contribution of $\tilde{e}_L$ exchange is much smaller. From the polarization dependence one can obtain information on the mixing states of the neutralinos and on the masses of the exchanged selectrons. We have also studied the cross sections of chargino production, $e^+e^- \to \tilde{\chi}_i^+\tilde{\chi}_j^-$. By a suitable choice of the e^- and e^+ beam polarizations the relative importance of the s–channel or t–channel contributions can be enhanced. In this way information on the mixing states of the charginos and the mass of the exchanged $\tilde{\nu}_e$ can be obtained. For further results on neutralino and chargino production we refer to [1,5,6,7] and the references therein.

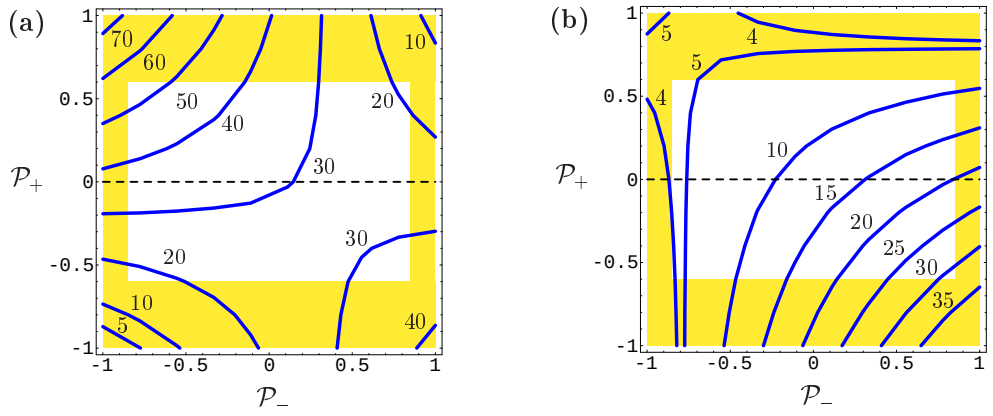

Figure 1: Contour lines of the cross section $\sigma(e^+e^- \to \tilde{\chi}_1^0\tilde{\chi}_2^0)$ at $\sqrt{s} = 230$ GeV for $m_{\tilde{\chi}_1^0} = 71$ GeV, $m_{\tilde{\chi}_2^0} = 130$ GeV, the other parameters as in text. The e^- (e^+) beam polarization is denoted by $\mathcal{P}_-$ ($\mathcal{P}_+$). The white region is for $|\mathcal{P}_-| \leq 85\%$, $|\mathcal{P}_+| \leq 60\%$.

3 Sfermion Production

In the discussion of third generation sfermions various aspects of left–right mixing are important. For each sfermion of definite flavour the interaction states $\tilde{f}_L$ and $\tilde{f}_R$ are mixed by Yukawa terms. Left–right mixing of the sfermions is described by the symmetric 2×2 mass matrices which depend on the soft SUSY–breaking mass parameters $M_{\tilde{Q}}$, $M_{\tilde{U}}$ etc., and the trilinear scalar coupling parameters A_t, A_b etc. (for details see [8,2,9]). The mass eigenstates are $\tilde{f}_1 = \tilde{f}_L \cos\theta_{\tilde{f}} + \tilde{f}_R \sin\theta_{\tilde{f}}$, $\tilde{f}_2 = \tilde{f}_R \cos\theta_{\tilde{f}} - \tilde{f}_L \sin\theta_{\tilde{f}}$, with $\theta_{\tilde{f}}$ the sfermion mixing angle. Strong $\tilde{f}_L - \tilde{f}_R$ mixing is expected for the third generation sfermions, because in this case the Yukawa couplings can be large. The experimental search for the third generation sfermions will be

particularly interesting at an e^+e^- linear collider, where precise measurements of masses, cross sections and decay branching ratios will be possible [10]. This will allow us to obtain information on the fundamental soft SUSY–breaking parameters.

The reaction $e^+e^- \to \tilde{f}_i\bar{\tilde{f}}_j$ proceeds via γ and Z exchange in the s–channel. The $\tilde{f}_i$ couplings depend on the sfermion mixing angle $\theta_{\tilde{f}}$. In Figs. 2 a, b we show the contour lines of the cross section $\sigma(e^+e^- \to \tilde{t}_1\bar{\tilde{t}}_1)$ as a function of the e^- and e^+ beam polarizations $\mathcal{P}_-$ and $\mathcal{P}_+$ at $\sqrt{s} = 500$ GeV for $m_{\tilde{t}_1} = 200$ GeV and two values of $\cos\theta_{\tilde{t}}$: $\cos\theta_{\tilde{t}} = 0.4$ in (a) and $\cos\theta_{\tilde{t}} = 0.66$ in (b). We have included initial–state radiation (ISR) and SUSY–QCD corrections (for details see [2,9]). The white windows show the range of polarizations $|\mathcal{P}_-| < 0.9$ and $|\mathcal{P}_+| < 0.6$. As one can see, one can significantly increase the cross section by using the maximally possible e^- *and* e^+ polarization. Moreover, beam polarization strengthens the $\cos\theta_{\tilde{t}}$ dependence and can thus be essential for determining the mixing angle. We have also calculated the cross sections for the production of sbottoms, staus and τ–sneutrinos. The results are in [2].

We have estimated the precision one may obtain for the parameters of the $\tilde{t}$ sector from

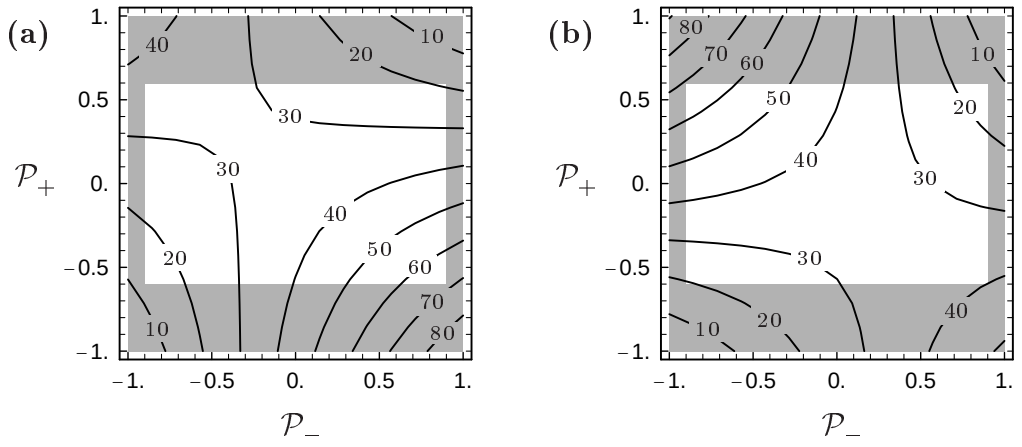

Figure 2: Dependence of $\sigma(e^+e^- \to \tilde{t}_1\bar{\tilde{t}}_1)$ on degree of electron and positron polarization at $\sqrt{s} = 500$ GeV, for $m_{\tilde{t}_1} = 200$ GeV, $\cos\theta_{\tilde{t}} = 0.4$ in (a) and $\cos\theta_{\tilde{t}} = 0.66$ in (b).

cross section measurements. We use the parameter point $m_{\tilde{t}_1} = 200$ GeV, $\cos\theta_{\tilde{t}} = -0.66$ as an illustrative example: For 90% left–polarized electrons (and unpolarized positrons) we have $\sigma_L(\tilde{t}_1\bar{\tilde{t}}_1) = 44.88$ fb, including SUSY–QCD, Yukawa coupling, and ISR corrections. For 90% right–polarized electrons we have $\sigma_R(\tilde{t}_1\bar{\tilde{t}}_1) = 26.95$ fb. According to the Monte Carlo study of [11] one can expect to measure the $\tilde{t}_1\bar{\tilde{t}}_1$ production cross sections with a statistical error of $\Delta\sigma_L/\sigma_L = 2.1\,\%$ and $\Delta\sigma_R/\sigma_R = 2.8\,\%$ in case of an integrated luminosity of $\mathcal{L} = 500$ fb^{-1} (i.e. $\mathcal{L} = 250$ fb^{-1} for each polarization). Scaling these values to $\mathcal{L} = 100$ fb^{-1} leads to $\Delta\sigma_L/\sigma_L = 4.7\,\%$ and $\Delta\sigma_R/\sigma_R = 6.3\,\%$. Figure 3 a shows the corresponding error bands and error ellipses in the $m_{\tilde{t}_1}$–$\cos\theta_{\tilde{t}}$ plane. The resulting errors on the stop mass and mixing angle are: $\Delta m_{\tilde{t}_1} = 2.2$ GeV, $\Delta\cos\theta_{\tilde{t}} = 0.02$ for $\mathcal{L} = 100$ fb^{-1} and $\Delta m_{\tilde{t}_1} = 1.1$ GeV, $\Delta\cos\theta_{\tilde{t}} = 0.01$ for $\mathcal{L} = 500$ fb^{-1}. With the additional use of a 60% polarized e^+ beam these values can still be improved by $\sim 25\%$.

For the determination of the mixing angle, one can also make use of the left–right asymmetry A_{LR}. At $\sqrt{s} = 500$ GeV we get $A_{LR}(e^+e^- \to \tilde{t}_1\bar{\tilde{t}}_1) = 0.2496$ for the parameter point chosen and 90% polarized electrons. Taking into account experimental errors as determined in [11], a theoretical uncertainty of 1%, and $\delta P/P = 10^{-2}$ we get $\Delta A_{LR} = 2.92\%$ (1.16%) for $\mathcal{L} = 100\,\text{fb}^{-1}$ ($500\,\text{fb}^{-1}$). This corresponds to $\Delta\cos\theta_{\tilde{t}} = 0.0031$ (0.0012). This is most likely the most precise method to determine the stop mixing angle. The corresponding error bands are shown in Fig. 3 b.

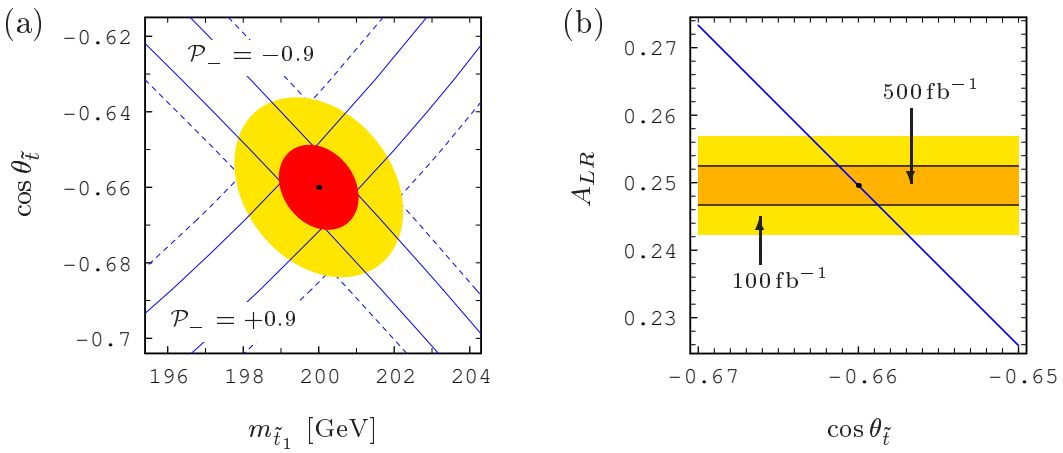

Figure 3: (a) Error bands and 68% CL error ellipse for determining $m_{\tilde{t}_1}$ and $\cos\theta_{\tilde{t}}$ from cross section measurements; the dashed lines are for $\mathcal{L} = 100$ fb^{-1} and the full lines for $\mathcal{L} = 500$ fb^{-1}. (b) Error bands for the determination of $\cos\theta_{\tilde{t}}$ from A_{LR}. In both plots $m_{\tilde{t}_1} = 200$ GeV, $\cos\theta_{\tilde{t}} = -0.66$, $\sqrt{s} = 500$ GeV, $\mathcal{P}_- = \pm 0.9$, $\mathcal{P}_+ = 0$.

Acknowledgements

A. B. is grateful to Prof. Tran Thanh Van and the organizers of the IVth Rencontres du Vietnam for creating an inspiring atmosphere at this conference. This work was supported in part by the "Fonds zur Förderung der Wissenschaftlichen Forschung of Austria", project no. P13139-PHY. W.P. is supported by the Spanish "Ministerio de Educacion y Cultura" under the contract SB97-BU0475382, by DGICYT grant PB98-0693, and by the TMR contract ERBFMRX-CT96-0090.

References

1. G. Moortgat–Pick, A. Bartl, H. Fraas, W. Majerotto, LC-TH-2000-032, hep-ph/0002253; LC-TH-2000-033, hep-ph/0004181; DESY 00-098, hep-ph/0007222.
2. A. Bartl, H. Eberl, S. Kraml, W. Majerotto, W. Porod, LC-TH-2000-031, hep-ph/0002115.
3. H.P. Nilles, *Phys. Rep.* **110**, 1 (1984); H.E. Haber, G.L. Kane, *Phys. Rep.* **117**, 75 (1985).
4. A. Bartl, H. Fraas, W. Majerotto, *Z. Phys.* C **30**, 441 (1986); *Nucl. Phys.* B **278**, 1 (1986); A. Bartl, H. Fraas, W. Majerotto, N. Oshimo, *Phys. Rev.* D **40**, 1594 (1989); A. Bartl, H. Fraas, W. Majerotto, B. Mößlacher, *Z. Phys.* C **55**, 257 (1992).
5. Talk by J. Kalinowski, these Proceedings; S. Y. Choi, M. Guchait, J. Kalinowski, P. M. Zerwas, hep-ph/0001175; S. Y. Choi, A. Djouadi, M. Guchait, J. Kalinowski, H. S. Song, P. M. Zerwas, hep-ph/0002033.
6. Talk by J. L. Kneur, these Proceedings; J. L. Kneur, G. Moultaka, *Phys. Rev.* D **59**, 015005 (1999).
7. G. Moortgat–Pick, PhD Thesis, Würzburg 1999, ISBN 3-8265-6981-4; G. Moortgat–Pick, H. Fraas, A. Bartl, W. Majerotto, *Eur. Phys. J.* C **7**, 1999 (1999); *Eur. Phys. J.* C **9**, 521 (1999);
8. J. F. Gunion, H. E. Haber, *Nucl. Phys.* B **272**, 1 (1986).
9. W. Porod, doctoral thesis, Univ. Vienna 1997, hep-ph/9804208; S. Kraml, doctoral thesis, TU Vienna 1999, hep-ph/9903257; A. Bartl, H. Eberl, S. Kraml, W. Majerotto, W. Porod, A. Sopczak, *Z. Phys.* C **76**, 76 (1997); H. Eberl, A. Bartl, W. Majerotto, *Nucl. Phys.* B **472**, 481 (1996); H. Eberl, S. Kraml, W. Majerotto, *JHEP* **9905**, 016 (1999).
10. E. Accomando et al., *Phys. Rep.* **299**, 1 (1998).
11. M. Berggren, R. Keranen, H. Nowak, A. Sopczak, hep-ph/9911345.